



Reshaping the tumor microenvironment with oncolytic viruses, positive regulation of the immune synapse, and blockade of the immunosuppressive oncometabolic circuitry

Teresa T Nguyen,^{1,2} Dong Ho Shin,^{1,2} Sagar Sohoni ,¹ Sanjay K Singh,³ Yisel Rivera-Molina,¹ Hong Jiang ,¹ Xuejun Fan,¹ Joy Gumin,³ Frederick F Lang,³ Christopher Alvarez-Breckenridge,³ Filipa Godoy-Vitorino,⁴ Lisha Zhu,⁵ W Jim Zheng,⁵ Lijie Zhai,⁶ Erik Ladomersky,⁶ Kristen L Lauing,⁶ Marta M Alonso ,^{7,8} Derek A Wainwright ,^{6,9} Candelaria Gomez-Manzano,^{1,2} Juan Fueyo ^{1,2}

To cite: Nguyen TT, Shin DH, Sohoni S, *et al.* Reshaping the tumor microenvironment with oncolytic viruses, positive regulation of the immune synapse, and blockade of the immunosuppressive oncometabolic circuitry. *Journal for ImmunoTherapy of Cancer* 2022;**10**:e004935. doi:10.1136/jitc-2022-004935

► Additional supplemental material is published online only. To view, please visit the journal online (<http://dx.doi.org/10.1136/jitc-2022-004935>).

Accepted 27 June 2022



© Author(s) (or their employer(s)) 2022. Re-use permitted under CC BY-NC. No commercial re-use. See rights and permissions. Published by BMJ.

For numbered affiliations see end of article.

Correspondence to

Dr Juan Fueyo;
jfueyo@mdanderson.org

Dr Candelaria Gomez-Manzano;
cmanzano@mdanderson.org

ABSTRACT

Background Oncolytic viruses are considered part of immunotherapy and have shown promise in preclinical experiments and clinical trials. Results from these studies have suggested that tumor microenvironment remodeling is required to achieve an effective response in solid tumors. Here, we assess the extent to which targeting specific mechanisms underlying the immunosuppressive tumor microenvironment optimizes viroimmunotherapy. **Methods** We used RNA-seq analyses to analyze the transcriptome, and validated the results using Q-PCR, flow cytometry, and immunofluorescence. Viral activity was analyzed by replication assays and viral titration. Kyn and Trp metabolite levels were quantified using liquid chromatography–mass spectrometry. Aryl hydrocarbon receptor (AhR) activation was analyzed by examination of promoter activity. Therapeutic efficacy was assessed by tumor histopathology and survival in syngeneic murine models of gliomas, including Indoleamine 2,3-dioxygenase (IDO)^{-/-} mice. Flow cytometry was used for immunophenotyping and quantification of cell populations. Immune activation was examined in co-cultures of immune and cancer cells. T-cell depletion was used to identify the role played by specific cell populations. Rechallenge experiments were performed to identify the development of anti-tumor memory.

Results Bulk RNA-seq analyses showed the activation of the immunosuppressive IDO-kynurenine-AhR circuitry in response to Delta-24-RGDOX infection of tumors. To overcome the effect of this pivotal pathway, we combined Delta-24-RGDOX with clinically relevant IDO inhibitors. The combination therapy increased the frequency of CD8⁺ T cells and decreased the rate of myeloid-derived suppressor cell and immunosuppressive Treg tumor populations in animal models of solid tumors. Functional studies demonstrated that IDO-blockade-dependent activation of immune cells against tumor antigens could be reversed by the oncometabolite kynurenine. The concurrent targeting of the effectors and suppressors of

WHAT IS ALREADY KNOWN ON THIS TOPIC

⇒ Oncolytic viruses are promising antiglioma agents. We have reported that 20% of patients with glioma treated with a single intratumoral injection of an oncolytic adenovirus underwent complete or partial responses; however, in addition to driving an anti-tumor immune response, the infection of a tumor elicits the resurface of an immunosuppressive environment that opposes and counteracts the tumor eradication of the tumor.

WHAT THIS STUDY ADDS

⇒ In this work, we combined an oncolytic virus, which carries a positive activator of T-cells, with the inhibition of the Indoleamine 2,3-dioxygenase (IDO) cascade, a key player in the tumor immunosuppressive environment. This therapeutic strategy reshaped the tumor microenvironment in favor of an anti-tumor immune response and prolonged the survival of glioma-bearing mice.

HOW THIS STUDY MIGHT AFFECT RESEARCH, PRACTICE, OR POLICY

⇒ According to our data, the design of future clinical trials with oncolytic adenoviruses should consider the addition of IDO inhibitors to enhance the immune-mediated aspect of the antitumor effect.

the tumor immune landscape significantly prolonged the survival in animal models of orthotopic gliomas.

Conclusions Our data identified for the first time the *in vivo* role of IDO-dependent immunosuppressive pathways in the resistance of solid tumors to oncolytic adenoviruses. Specifically, the IDO-Kyn-AhR activity was responsible for the resurface of local immunosuppression and resistance to therapy, which was ablated through IDO inhibition. Our data indicate that combined molecular and immune

therapy may improve outcomes in human gliomas and other cancers treated with virotherapy.

INTRODUCTION

Natural human viral infections can induce remission in several types of cancers. During the pandemic, patients with cancer infected with SARS-CoV-2 have experienced complete remissions,¹² illustrating the antitumor capacity of viruses. In one phase I study, the oncolytic virus Delta-24-RGD (DNX-2401) induced complete tumor regression in 20% of patients with recurrent glioblastoma.³ Other findings in this clinical trial, including radiological signs of inflammation, pseudoprogression, and tumor infiltration by T-bet⁺ CD8⁺ T cells, strongly suggested that the antitumor effects of Delta-24-RGD were due in part to an antitumor immune response. These observations agreed with preclinical studies showing that Delta-24-RGD infection induces autophagy and immunogenic cell death in glioblastoma.⁴⁵ To enhance the immune arm of this oncolytic virotherapy, we generated Delta-24-RGDOX (DNX-2440), a third-generation adenovirus that includes the T cell activator OX40-ligand (OX40L)⁶⁷ in the backbone of Delta-24-RGD. Preclinical studies have shown that Delta-24-RGDOX induces a stronger T cell-mediated antitumor effect than parental Delta-24-RGD in glioblastoma and metastatic melanoma murine models.⁶⁷ Based on these preclinical results, Delta-24-RGDOX is now being tested in clinical trials for the treatment of malignant gliomas (NCT03714334) and liver metastases (NCT04714983).

Infection of tumors with viruses is an efficient method of recruiting cytotoxic CD8⁺ T cells³⁶⁷; however, suppressive mechanisms within the tumor microenvironment restrain the effector immune response.⁸ Therefore, improving the overall potency of virotherapy may require targeting inherent tumor immunosuppression while augmenting T cell activation. Notably, viral infections elicit immunosuppressive mechanisms that further hinder virus-induced antitumor responses.⁹

Indoleamine 2,3-dioxygenase (IDO) is expressed in the tumor microenvironment and induces immune privilege, an effect that is reversed by the administration of IDO inhibitors.¹⁰ The catabolism of tryptophan (Trp) by IDO produces kynurenine (Kyn), a direct activator of aryl hydrocarbon receptor (AhR), promoting robust immunosuppression.¹¹¹² The IDO-Kyn-AhR multicellular circuitry plays a fundamental role at the center of the immune synapse and acts as a bridge among the main immune cell populations in tumors.¹³

Activation of the IDO cascade is a major characteristic of several tumors,^{14–16} including gliomas,¹⁷ and correlates with poor prognoses.¹⁷¹⁸ In addition to its role in tumors, IDO is activated in various tissues and cell subsets following cytokine stimulation during infection.¹⁹ Several clinical trials are examining IDO inhibitors as anticancer drugs. Most of these inhibitors (epacadostat, BMS-986205, navoximod, KHK2455, and BGB-7204) are direct IDO enzymatic inhibitors, whereas indoximod is a Trp

mimetic that imitates an artificial Trp-sufficiency signal on immune cells in an attempt to reverse IDO pathway-mediated suppression.²⁰²¹

Combinations of therapeutic strategies are probably required to overcome treatment resistance and improve the efficacy of immunotherapies in solid tumors. The main objective of this work was to determine the therapeutic efficacy and immune effects of combined treatment with Delta-24-RGDOX and IDO inhibitors in solid tumors. We showed that simultaneous activation of the effector arm of the immune system, using oncolytic viruses and OX40-mediated T cell activation, and inhibition of the suppressor arm, with IDO inhibitors, produced robust remodeling of the tumor microenvironment, significantly enhancing viroimmunotherapy and leading to tumor eradication in immunocompetent animal models.

METHODS

Methods are included in online supplemental materials.

RESULTS

Delta-24-RGDOX infection results in robust transcriptional modulation of the tumor microenvironment

Solid tumors consist of both tumor-intrinsic and tumor-extrinsic phenotypic features, which shape the overall tumor microenvironment. RNA sequencing (RNA-seq) enables the unbiased cellular and molecular profiling of complex tissues to dissect intratumoral heterogeneity. Leveraging this approach, we performed bulk RNA-seq analyses of Delta-24-RGDOX-infected murine gliomas to comprehensively examine changes in the tumor transcriptome. These data showed drastic reshaping of the tumor microenvironment following intratumoral infection (figure 1A,B). Specifically, ingenuity pathway analysis (IPA) of Delta-24-RGDOX-infected tumors showed an enhancement of inflammation-related canonical pathways in these tumors compared with control tumors (figure 1C). We also performed IPA to identify altered upstream regulators in tumor treated with Delta-24-RGDOX infection. This analysis identified IFN γ , TNF, IL1B, IFN α , and STAT1 as candidate regulators of the transcriptional response to Delta-24-RGDOX infection (figure 1D). With respect to estimated nontumor cell type abundances inferred from bulk tissue transcriptomes, the main impact was a remarkable increase in the CD8⁺ T cell proportion ($p=0.0031$) (figure 1E). Indirectly implying that the effects on these cell populations were specific, Delta-24-RGDOX infection resulted in a negligible effect on the transcriptional signatures of macrophages and dendritic cells. These data agreed with changes in the immune populations observed in murine models of glioma and melanoma on infection with oncolytic adenoviruses,⁶⁷ as well as those observed in surgical specimens from gliomas infected with Delta-24-RGD.³

Based on the rationale that IDO is triggered by IFN γ ²² and upregulated during viral infections,⁹ we asked

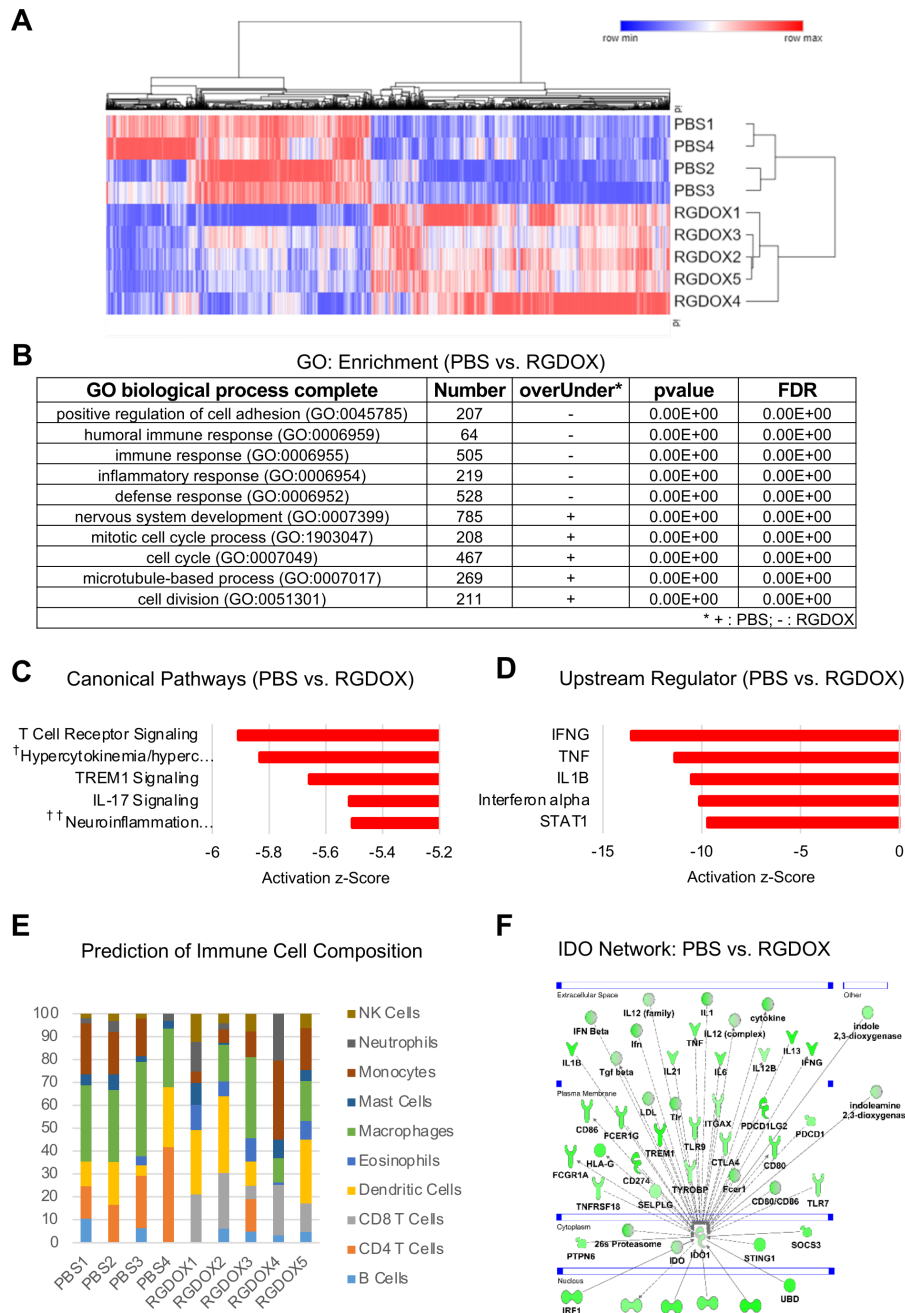


Figure 1 Delta-24-RGDOX treatment remodels the tumor microenvironment. Differentially expressed genes in tumors treated with PBS versus tumors treated with Delta-24-RGDOX were used for clustering, gene ontology (GO) biological process enrichment analysis, and pathway and network analyses. Analyses of tumors were performed on day 12, 5 days after the first dose of Delta-24-RGDOX. (A) Heatmap comparing the transcriptional signatures of intracranial GL261-5-derived tumors treated with PBS or Delta-24-RGDOX. The log₂-normalized expression levels of genes with significant adjusted p values (<0.05) across samples are shown. The color scale is shown above the heatmap. (B) GO biological process enrichment results for tumors treated with PBS or Delta-24-RGDOX. The five most significant GO biological processes are shown. GO biological processes significantly associated with PBS-treated tumors are marked as '+', whereas those significantly associated with Delta-24-RGDOX-treated tumors are marked as '-'. (C) The five most significantly altered canonical pathways in tumors treated with PBS vs Delta-24-RGDOX. Activation z-scores are plotted in the graph. †Hypercytokinemia/hyperchemokinemias in the pathogenesis of influenza; ††neuroinflammation signaling pathway. (D) The five most significantly altered upstream regulators in tumors treated with PBS versus Delta-24-RGDOX. Activation z-scores are plotted in the graph. The negative z-scores represent activation in Delta-24-RGDOX. (E) The prediction of the immune cell composition in GL261-5-derived brain tumors treated with PBS or Delta-24-RGDOX. The percentages of various immune cell populations in each sample are presented in the graph. The color code for the various immune cell types is shown to the right of the graph. (F) IDO1 network genes with significantly altered expression levels in tumors treated with PBS or Delta-24-RGDOX. The color intensity indicates the log₂ fold-change (green=activation) levels for each gene in PBS-treated tumors vs Delta-24-RGDOX-treated tumors. IDO, indoleamine 2,3-dioxygenase.

whether Delta-24-RGDOX treatment induces upregulation of the IDO network. We observed that a great number of IDO-related transcripts were upregulated after viroimmunotherapy, including those playing a pivotal role in maintaining glioma immunosuppression such as TGF β , CTLA-4, PD-1, and GATA-3 (figure 1F).

Collectively, these analyses indicated that Delta-24-RGDOX induced a robust effect on the tumor microenvironment. The pleiotropic impact of Delta-24-RGDOX infection includes not only the expected activation of proinflammatory pathways but also negative impacts on regulators of the immune responses against viruses and tumors. Within the negative regulatory network, IDO-related pathway is activated by Delta-24-RGDOX infection and appears to play a critical role in the re-emergence of the immunosuppressive response.

Delta-24-RGDOX elicits IDO expression and activation in gliomas

We next aimed to confirm the effect of Delta-24-RGDOX on the activity of the IDO pathway by assessing the production of IDO-related metabolites, such as Kyn, and the expression of key downstream targets of IDO, including the transcription factor AhR.^{22–24} Several proteins that are directly or indirectly activated by adenovirus infection via activation of cytokines can modulate IDO expression. Of note, IDO was the first gene discovered to be inducible by IFN γ ,²⁵ a potent mediator of antiviral immune responses. In addition, IDO is regulated by other molecular mechanisms activated during infection, such as the JAK/STAT²⁶ and IFN type I transduction signaling pathways.^{27–29}

In *in vitro* experiments, we observed a remarkable increase in IDO expression in human and murine glioma cells following treatment with IFN γ (online supplemental figure S1). We also determined that infection of GL261-5 and GSC-005 murine glioma cells with Delta-24-RGDOX triggered a sixfold to sevenfold increase in IDO levels, as assessed by qRT-PCR (figure 2A). Additionally, infection of intracranial GL261-5-derived gliomas with Delta-24-RGDOX led to a significant increase in IDO levels *in vivo*, and we observed a similar pattern in orthotopically implanted breast tumors (figure 2B,C).

Kyn is a product of the metabolic activity of IDO,³⁰ and therefore, we next sought to ascertain whether infection of murine tumors with Delta-24-RGDOX increased the production of this oncogenic metabolite *in vivo*. In agreement with the increased IDO mRNA expression observed in murine glioma cell lines on viral infection, both GL261-5- and GSC-005-derived tumors infected with Delta-24-RGDOX showed a significantly higher Kyn/Trp ratio than control mouse brain tumors (figure 2D), as determined by liquid chromatography-mass spectrometry, indicating the presence of an active IDO cascade in these tumors.

The IDO-mediated catabolism of Trp and subsequent production of Kyn suggested the potential activation of AhR, a key downstream target of IDO directly activated by Kyn.^{11 31} Importantly, AhR has dual functions as a

transcriptional target for immune escape by viruses^{32 33} and a promoter of immunosuppression in solid tumors, including gliomas.^{34–37} Using AhR reporter cells expressing a luciferase reporter functionally linked to an AhR-responsive promoter, we assessed the transcriptional activity of AhR in a panel of human glioma cell lines using supernatant of infected cells. We found that Delta-24-RGDOX treatment significantly increased AhR transcriptional activity (figure 2E), suggesting the treatment with the oncolytic adenovirus will have an effect on the IDO-Kyn-AhR pathway in infected cells and, multiplying the initial effect, in neighboring cells. Because the binding of Kyn to AhR promotes AhR translocation to the nucleus,³⁴ we analyzed the expression and subcellular localization of AhR in cancer cells infected with Delta-24-RGDOX using immunofluorescence. Compared with uninfected cells, infected cells showed significant increases in the whole-cell and nuclear intensity of AhR as well as a remarkable increase in the percentage of cells displaying nuclear AhR (figure 2F–H). Importantly, the Delta-24-RGDOX-mediated changes were similar to the subcellular trafficking of AhR observed when uninfected cultures were treated with Kyn (figure 2F–H).

These results suggested that following Delta-24-RGDOX infection, there was substantial activation of the immunosuppressive IDO-Kyn-AhR cascade. The increased expression of the oncometabolite Kyn and upregulation of the transcriptional activity of AhR strongly suggested that infection of a tumor is followed by activation of the IDO circuitry with subsequent maintenance of an immunosuppressive environment.

The Delta-24-RGDOX replication capability and cytotoxic effect are preserved under IDO inhibition

To ascertain the effect of IDO activity specifically on virus oncolytic activity, we assessed the viral infectivity, viral replication, and virus-induced cytopathic effect of Delta-24-RGDOX in a panel of human and murine glioma cell lines (online supplemental figure S2). We observed that treating glioma cultures with a direct IDO enzyme inhibitor did not modify the activity of Delta-24-RGDOX in any of the human or murine cancer cell lines tested. Thus, the quantitative levels of progeny virion production and expression of viral proteins were unchanged during IDO inhibition (online supplemental figure 3A,B,F,G). Corroborating these results, a timepoint analysis of cell viability showed that the oncolytic effect was similar in cells treated with Delta-24-RGDOX alone or in combination with IDO inhibitors (online supplemental figure 3C,D,E,H,I). These results suggested that the potency of Delta-24-RGDOX remained unchanged under conditions of IDO inhibition.

The combination of Delta-24-RGDOX and IDO inhibitors enhances immune activation in murine models of glioma

To determine the phenotypic changes within the tumor microenvironment following the combined administration of Delta-24-RGDOX and an IDO inhibitor, we

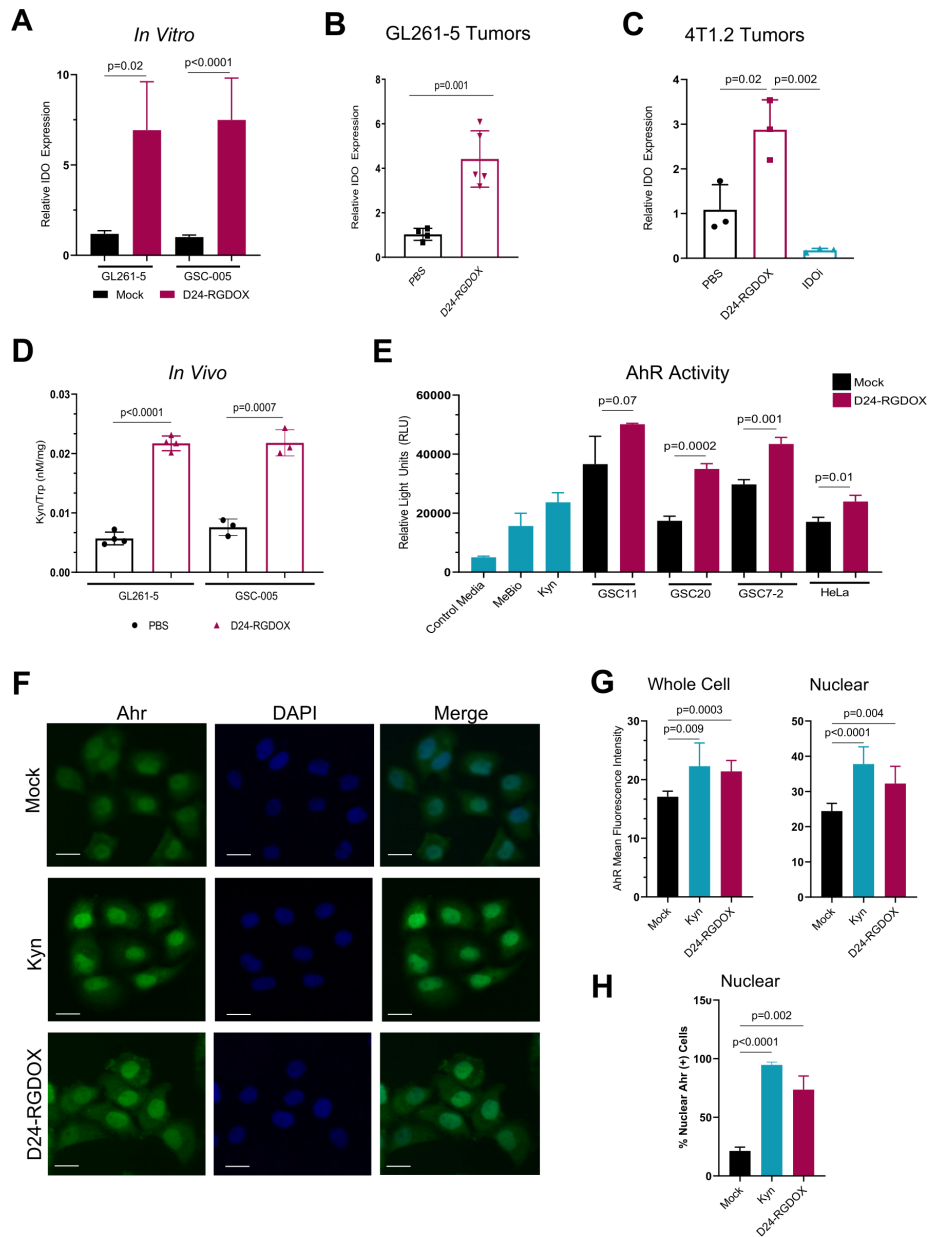


Figure 2 Oncolytic adenoviruses induce the expression and activation of the IDO-Kyn-AhR cascade *in vivo* and *in vitro*. (A) IDO expression in GL261-5 and GSC-005 murine glioma cells in response to Delta-24-RGDOX infection. Cells were infected with Delta-24-RGDOX (100–150 multiplicities of infection (MOIs)) over 48 hours. RNA was extracted, and the relative levels of IDO were measured using qRT-PCR; GAPDH or β -Actin was used as a housekeeping gene control. The column graph shows $2^{-\Delta(\text{Ct}^{\text{GAPDH}} - \text{Ct}^{\text{IDO}})}$ results normalized to the mock-infected control. (B, C) Relative IDO expression in GL261-5 or 4T1.2 tumors in response to oncolytic adenovirus treatment *in vivo*. In (B, D), the mice were implanted intracranially with GL261-5 or GSC-005 cells and intratumorally treated with PBS or Delta-24-RGDOX; brain tumors were collected and flash-frozen on day 12. In (C), the mice were implanted with 4T1.2 cells in the right mammary fat pad and treated with PBS, D24-RGDOX, or indoximod (IDOi); tumors were collected and flash-frozen on day 36. RNA was extracted and analyzed as described in (A). (D) The Kyn and Trp metabolite levels in murine gliomas following the indicated treatments (described in (B)) were quantified using liquid chromatography–mass spectrometry. Data are presented as the ratios \pm SDs of Kyn concentrations to Trp concentrations. (E) AhR activity in human GSC lines and HeLa cells in response to Delta-24-RGDOX infection. Cells were mock-infected or infected with Delta-24-RGDOX (50 MOI) over 48 hours, and the transcriptional activity of AhR in the cells was quantified by evaluating the supernatants. Controls included medium (negative), medium containing the AhR agonist MeBio (0.32 nM), and medium containing Kyn (25 μ M). HeLa cells were used as a positive control. (F) AhR expression and nuclear translocation on Delta-24-RGDOX treatment. HeLa cells were infected with Delta-24-RGDOX (25 MOI) over 48 hours or treated with Kyn (positive control) and then immunostained for AhR detection. Representative images of AhR-FITC staining, DAPI (nuclear) staining, and merged FITC/DAPI staining are shown. Scale bars, 50 μ m. (G) Quantification of the mean fluorescence intensity of AhR in whole cells and nuclear compartments. (H) Frequency of nuclear AhR-positive cells after the indicated treatments, as analyzed using ImageJ software. Data are shown as the means \pm SDs. P values were generated by using a two-tailed Student's t-test. AhR, aryl hydrocarbon receptor.

performed RNA-seq analysis of GL261-5 tumors from mice treated with PBS, an IDO inhibitor or Delta-24-RGDOX alone or in combination. Hierarchical clustering of genes and samples showed that the transcriptome signatures of PBS-treated and IDO inhibitor-treated mice were not different. In contrast, Delta-24-RGDOX infection resulted in significant alterations in gene pathways, making Delta-24-RGDOX-treated mice distinct from PBS- and IDO inhibitor-treated mice (figure 3A,C). There was also a clear difference in the global transcriptome signature between Delta-24-RGDOX- and combination therapy-treated mice (figure 3A,C). Furthermore, network analyses of differentially expressed genes demonstrated that the addition of IDO network inhibition to Delta-24-RGDOX infection reverted the effects of the adenovirus on several key immune-related transcripts that were induced during adenovirus infection, such as immune checkpoint regulators, inflammation-related cytokines, Toll-like receptors 7 and 9 and components of the stimulator of interferon genes (STING) pathway (figure 3C).

The predicted immune cell composition and transcriptome signature showed minimal differences between PBS-treated and IDO inhibitor-treated brain tumors (figure 3B). Interestingly, upon treatment with Delta-24-RGDOX, the estimated percentage of CD8⁺ T cells almost doubled compared with that in the group treated with IDO inhibition alone (Delta-24-RGDOX: 23.7%; IDO inhibitor: 12.0%; PBS: 16.3%); the combination of Delta-24-RGDOX and the IDO inhibitor did not show significant changes in the CD8⁺T cell transcriptome frequency compared with Delta-24-RGDOX alone (combination: 26.2%) (figure 3B).

The altered immune responses of combination therapy- versus Delta-24-RGDOX-treated mice confirmed and complemented the results that showed increased activation of the IDO network in Delta-24-RGDOX-treated mice. In this experiment, performed 14 days after the first viral administration, we did not observe the upregulation of the IDO transcript detected 5 days after viral treatment (figure 2), but the IDO network was still activated. Additionally, we observed a decrease in IDO pathway activation in tumors from combination therapy-treated mice compared to mice in the control group (figure 3C,D). These data also illustrated the ability of the IDO inhibitor to decrease the number of IDO-related transcripts induced in tumors infected with the adenovirus (figure 3D). Remarkably, the combination treatment decreased the expression of more than 90% of the upstream and downstream IDO-related transcripts induced on Delta-24-RGDOX treatment.

Together, these results indicate that the combination of IDO inhibition with Delta-24-RGDOX infection modulates the tumor microenvironment by two means, promoting an adaptive immune response while decreasing immunosuppression caused by virus-induced IDO pathway activation. These collective findings strengthen our rationale for combining Delta-24-RGDOX infection with IDO inhibition for the treatment of gliomas.

Combination of Delta-24-RGDOX infection with IDO inhibition prolongs the survival of glioma-bearing mice

The results from several clinical studies using oncolytic viruses,^{338–41} chimeric antigen receptor T cells,^{42–44} or anti-PD-1 and anti-PD-L1 antibodies^{45 46} have shown that single cancer immunotherapies are unlikely to circumvent the immune evasion mechanisms of gliomas. Therefore, we aimed to test a three-pronged therapy in immunocompetent animal models. First, to ascertain whether IDO inhibition impairs oncolytic ability *in vivo*, we treated GL261-5 tumor-bearing IDO-knockout (KO) mice with Delta-24-RGDOX. In this context of a genetically mediated IDO inhibition in the tumor microenvironment, Delta-24-RGDOX prolonged median survival and produced 20% long-term survivors (online supplemental figure S3). We then compared the survival of glioma-bearing IDO-KO mice and wild-type mice treated with Delta-24-RGDOX or PBS (figure 4A,B). As expected, all the PBS-treated mice succumbed to their tumors, with a median survival time of 44 days, regardless of the mouse genotype. Importantly, Delta-24-RGDOX treatment resulted in a longer median survival duration and a higher percentage of long-term survivors in the IDO-KO mice than in the wild-type mice ($p=0.0142$). To further determine the therapeutic efficacy of Delta-24-RGDOX combined with IDO inhibition, we tested this treatment in the intracranial GL261-5 tumor-bearing mouse model (figure 4C,D). The median survival times of the control-treated mice and the IDO inhibitor 1MT-treated mice were 38.5 and 37.5 days, respectively. As expected, the mice treated with Delta-24-RGDOX had significantly prolonged survival, with a median survival time of 46.5 days. In addition, 20% of the mice treated with Delta-24-RGDOX survived for 120 days (the last timepoint tested). Notably, mice treated with a combination of Delta-24-RGDOX and the IDO inhibitor had the greatest therapeutic benefit, with a median survival time of 108.5 days and a remarkable long-term survival (120 days) rate of 50% ($p=0.004$; vs Delta-24-RGDOX).

Next, we asked whether the antiglioma effect of the combined Delta-24-RGDOX and IDO inhibitor therapy is immune mediated. To address this question, we performed rechallenge experiments with long-term survivors in the combination therapy group using intracranial injection of GL261-5 cells into the contralateral hemisphere (figure 4C,E). As expected, treatment-naïve mice injected with GL261-5 cells died within 50 days, but the mice treated with Delta-24-RGDOX and the IDO inhibitor survived 100 days with no symptoms of disease. These data unequivocally indicated the immune nature of the treatment response, as the combination of Delta-24-RGDOX and IDO inhibitors generated immune memory against glioma antigens.

To confirm these results, we tested the combination therapy in another murine glioma model. To this end, we intracranially implanted GSC-005 cells in C57BL/6 mice and treated the mice with either PBS or Delta-24-RGDOX with or without the IDO inhibitor (figure 4C,F). In this case, we used BGB-7204, a clinical-grade CNS-penetrating

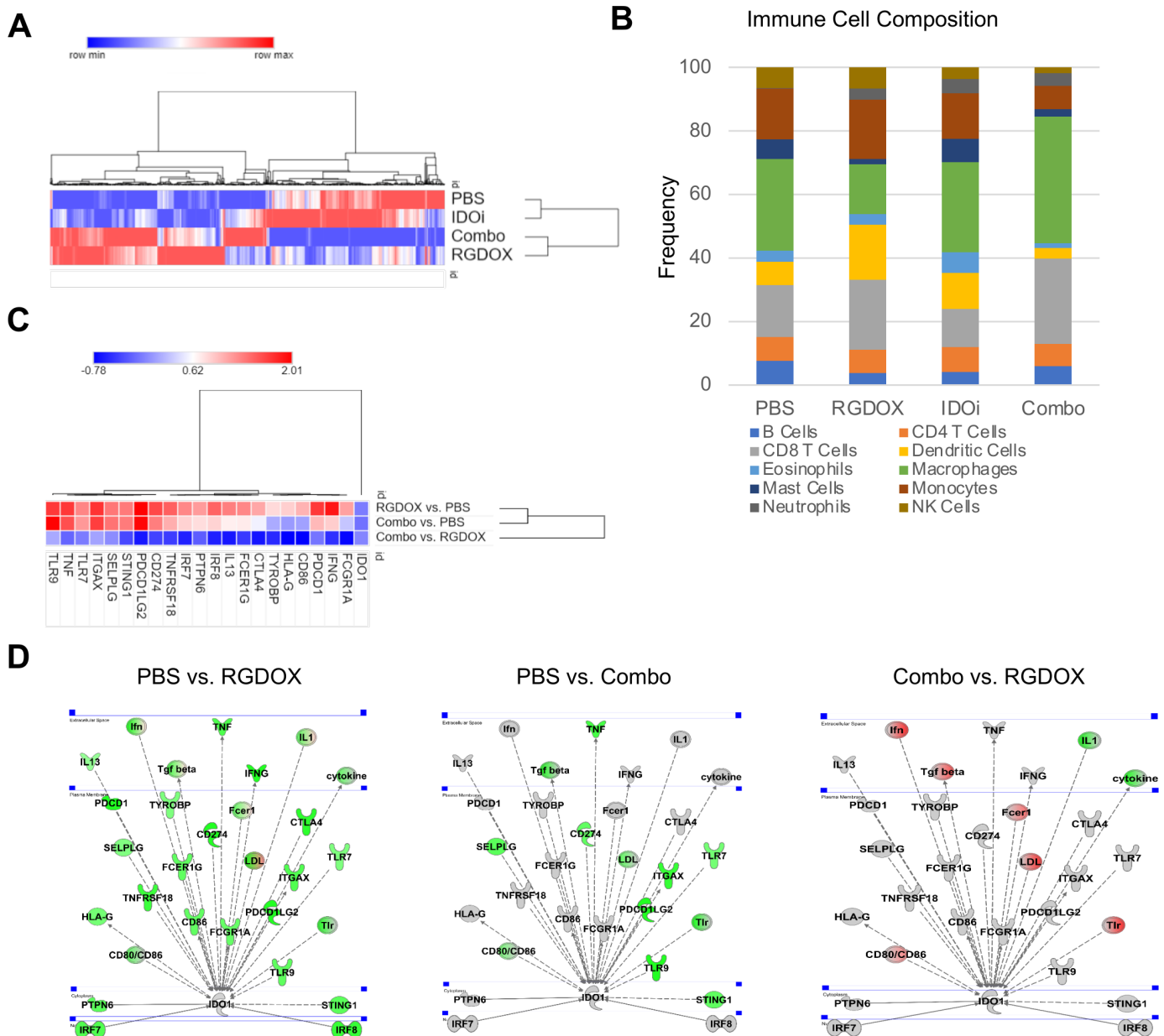


Figure 3 IDO inhibition modulates the tumor microenvironment of Delta-24-RGDOX-treated murine brain tumors. Differentially expressed genes in tumors treated with PBS, the IDO inhibitor (IDOi) indoximod, Delta-24-RGDOX (RGDOX), or the IDOi and Delta-24-RGDOX (combo) utilized for clustering, immune population prediction, and pathway and network analyses. Examination of tumors were performed on day 21, 14 days after the first dose of Delta-24-RGDOX. (A) Heatmap comparing the transcriptional signatures of intracranial GL261-5-derived tumors treated with PBS, the IDOi, Delta-24-RGDOX, or the combination therapy. Tumors were established in these mice for 21 days, and the mice underwent treatment for 14 days. The log₂-normalized averaged expression levels of genes with significant adjusted p values (<0.05) across sample groups are shown. The color scale is shown above the heatmap. (B) The prediction of the immune cell composition in GL261-5-derived brain tumors in the indicated treatment group. The percentages of various immune cell populations in each sample are presented in the graph. The color code for the various immune cell types is shown at the bottom of the graph. (C) Heatmap or (D) pathway representation of IDO1 network genes with significantly altered expression levels in tumors; treatment group comparisons are indicated, in the experiment delineated in (A). The color scale is shown above the heatmap. The color intensity of the pathway representation graphics indicates the log₂ fold-change levels for each gene in the specified treatment group comparison; gray represents unchanged, green represents activation, and red represents inhibition. IDO, indoleamine 2,3-dioxygenase.

IDO1 enzyme inhibitor.²⁰ The PBS-treated and IDO inhibitor-treated mice had median survival times of 38.5 or 42 days, respectively, and 100% of the mice died due to tumor growth. As expected, treatment of these brain

tumor-bearing mice with Delta-24-RGDOX prolonged survival compared with control treatment, with a median survival time of 53 days (p=0.02). Similar to the GL261-5 model, the GSC-005 tumor-bearing mice treated with the

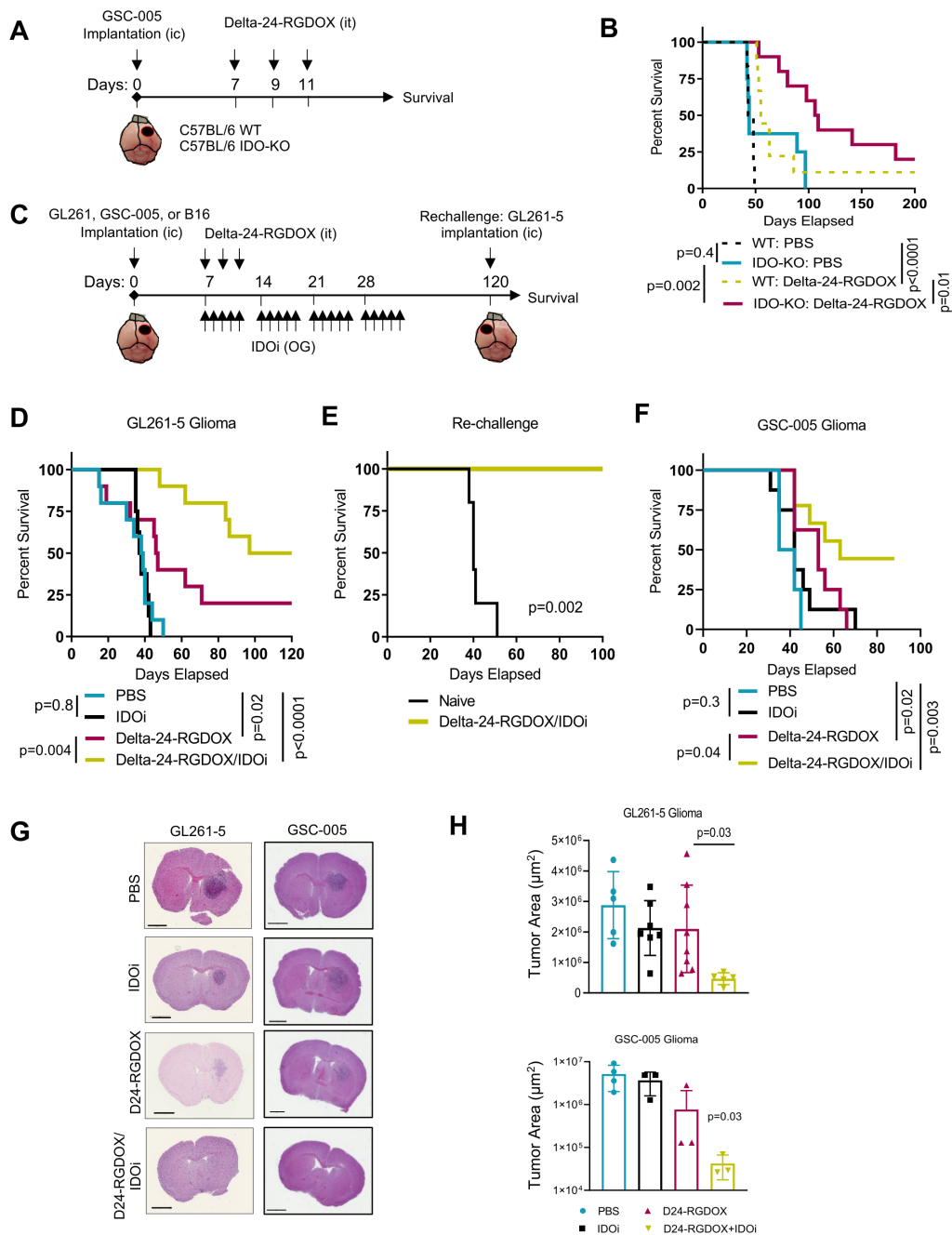


Figure 4 Combined treatment with Delta-24-RGDOX infection and IDO inhibition results in an enhanced therapeutic effect and tumor regression. (A) Treatment schedule of wild-type (WT) and IDO-KO C57BL/6 mice bearing intracranial (IC) GSC-005 tumors. GSC-005 cells were implanted IC on day 0, and the mice were randomly assigned to receive intratumoral (IT) injection of either Delta-24-RGDOX or vehicle. Survival was monitored for up to 200 days. (B) Kaplan-Meier survival curves of the mice included in the experiment depicted in (A). (C) Treatment schedule of C57BL/6 mice-bearing intracranial tumors that were treated with Delta-24-RGDOX alone or in combination with an IDO inhibitor (IDOi). OG, oral gavage. (D) Kaplan-Meier survival curves of intracranial GL261-5 tumor-bearing C57BL/6 mice treated with vehicle or with Delta-24-RGDOX alone, or in combination with the IDOi 1-methyl-DL-tryptophan (1MT; $n=10/\text{group}$). (E) Long-term survivors previously treated with the combination therapy described in (D) were rechallenged with an intracranial injection of GL261-5 cells into the contralateral hemisphere, and their survival was compared with that of control treatment-naïve mice ($n=5/\text{group}$). (F) Kaplan-Meier survival curves of intracranial GSC-005 tumor-bearing C57BL/6 mice treated with vehicle or with Delta-24-RGDOX alone or in combination with the IDOi BGB-7204 ($n=9\text{--}10/\text{group}$). (G, H) The brains of intracranial GL261-5 or GSC-005 tumor-bearing C57BL/6 mice were subjected to histopathological analyses on day 15 (GL261-5) or 24 (GSC-005) after treatment with PBS, Delta-24-RGDOX, indoximod, or the combination therapy ($n=5\text{--}8/\text{group}$). Representative images of H&E staining (G) and the average tumor surface areas (H) were acquired using Aperio ImageScope software. Scale bar, 2 mm. P values were derived with the log-rank test (B, D–F) and a two-tailed Student's t-test (G–I). The difference between the arms Delta-24-RGDOX and Delta-24-RGDOX+IDOi was calculated using the restricted mean survival Qme (RMST) to account for the long-term survivors. IDO, indoleamine 2,3-dioxygenase.

combination of Delta-24-RGDOX and the IDO inhibitor exhibited the longest median survival (63 days) and resulted in 44% long-term survivors, showing a significant long-term survival rate in comparison to Delta-24-RGDOX as a single treatment ($p=0.04$).

In agreement with the survival data, analysis of tissue sections of brains harvested from mice injected with either GL261-5 glioma cells or GSC-005 glioma cells in the different treatment groups showed progressive tumor regression in the mice treated with the combination therapy (figure 4G,H; online supplemental figures S4,S5). Of note, neither the GL261-5 nor GSC-005 brain tumor-bearing animals treated with the combination therapy exhibited significant changes in weight over the course of treatment, indicating the tolerability of this treatment (online supplemental figure S6).

In summary, antitumor treatment with the combination of Delta-24-RGDOX and an IDO inhibitor is superior to treatment with either agent alone and significantly prolongs survival, generates long-term survivors, and induces antiglioma immune memory in immunocompetent animal models of cancer.

The anticancer effect of combination treatment with Delta-24-RGDOX infection plus IDO inhibition is dependent on CD4⁺ T cell activity

To further understand the immune-mediated mechanisms underlying the anticancer effect of the combination of Delta-24-RGDOX infection plus IDO inhibition, we assessed the phenotypic changes in the lymphocyte population following treatment (figure 5A). Flow cytometric analyses revealed a significant influx of CD45⁺CD3⁺ T cells in both GL261-5 and GSC-005 tumor-bearing mice treated with Delta-24-RGDOX compared with control-treated mice (figure 5B). These results were confirmed with immunohistochemical assessments of CD3⁺ T cells in the two murine brain tumor models (figure 5C; online supplemental figure S7). Analysis of absolute counts of intratumoral CD3⁺, CD4⁺, and CD8⁺ T cell populations showed a significant difference among the treatment groups (figure 5B, D and E).

Based on our RNA-seq findings suggesting a link between IDO and an immunosuppressive tumor microenvironment following Delta-24-RGDOX infection and on previous reports of IDO activation resulting in increasing frequencies of regulatory T cells (Tregs) and myeloid-derived suppressor cells (MDSCs),⁴⁷ we next assessed whether these two cell populations underwent changes in treated tumors. Gene set enrichment analyses of RNA-seq data showed positive enrichment of gene sets associated with Tregs (normalized enrichment score of 1.375, $p=0.0$, FDR q value=0.0439) and MDSCs (normalized enrichment score of 1.352, $p=0.0$, FDR q -value=0.0642) in tumors treated with Delta-24-RGDOX compared with control-treated tumors (figure 5F, left panels). In contrast, the combination of Delta-24-RGDOX infection with IDO inhibition led to a reversal of these findings, shifting the tumor microenvironment

away from an immunosuppressive phenotype (figure 5F, right panels). These results were confirmed by flow cytometric analyses of the tumor microenvironment of virus-treated and combination-treated mice (figure 5G). Importantly, whereas Delta-24-RGDOX alone increased Treg and MDSC populations, Delta-24-RGDOX plus the IDO inhibitor significantly decreased these crucial immunosuppressive populations. Similar results were observed from the analysis of CD4⁺CD25⁺FoxP3⁺, which have been considered Tregs precursors^{48–49} (online supplemental figure S8).

Since CD4⁺ T cells constitute the target of the OX40 ligand/receptor synapse,⁵⁰ we aimed to understand the extent to which these cells contributed to the therapeutic efficacy of the combination of Delta-24-RGDOX infection and IDO inhibition in glioblastoma. In this case, we used Indoximod as IDO inhibitor, which is being tested in clinical trials. Our results showed that combination of Delta-24-RGDOX with Indoximod was more potent than the combination using 1MT (figure 4D). To analyze the role of CD4⁺ T cells, we performed these cells using anti-CD4 antibodies (figure 6A–C). Our results showed that in mice with a decreased population of CD4⁺ T cells, the antiglioma effect of the combination treatment was abolished, and the median survival of the combination-treated CD4⁺ T cell-depleted mice was similar to that of control-treated mice (figure 6D). This loss of the anticancer effect indicates that the combined therapy depends on the CD4⁺ T helper cell population to induce maximal anticancer effects and produce long-term survivors.

In summary, our data indicated that the combination of Delta-24-RGDOX infection with IDO inhibition resulted in intratumoral infiltration of several T cell populations, such as CD45⁺CD3⁺, CD45⁺CD3⁺CD4⁺ and CD45⁺CD3⁺CD8⁺ cells. Of interest, we detected paradoxical activation of immunosuppressive populations, including MDSCs and Tregs, by Delta-24-RGDOX, which was partially reversed by the addition of IDO inhibitors. Furthermore, the depletion of CD4⁺ cells, the main target of the OX40 ligand/receptor synapse,⁵⁰ abrogated the antitumor efficacy of this combination therapy. These findings underscored the critical role of the CD4⁺ T cell population in the eradication of tumors treated with Delta-24-RGDOX and an IDO inhibitor.

Treatment with Delta-24-RGDOX and IDO inhibition led to functional activation of antitumor immune cells

To study the immune response to treatment, we performed coculture-based functional immune assays. Splenocytes from GL261-5 tumor-bearing mice treated with Delta-24-RGDOX with or without IDO inhibitors were cocultured with uninfected or Delta-24-RGDOX-infected glioma cells to assess antitumor immune responses (figure 7A–D). We showed that splenocytes isolated from mice treated with the combination therapy displayed robust immune activation against Delta-24-RGDOX-infected glioma cells, as determined by measuring the secreted levels of the Th1 cytokines

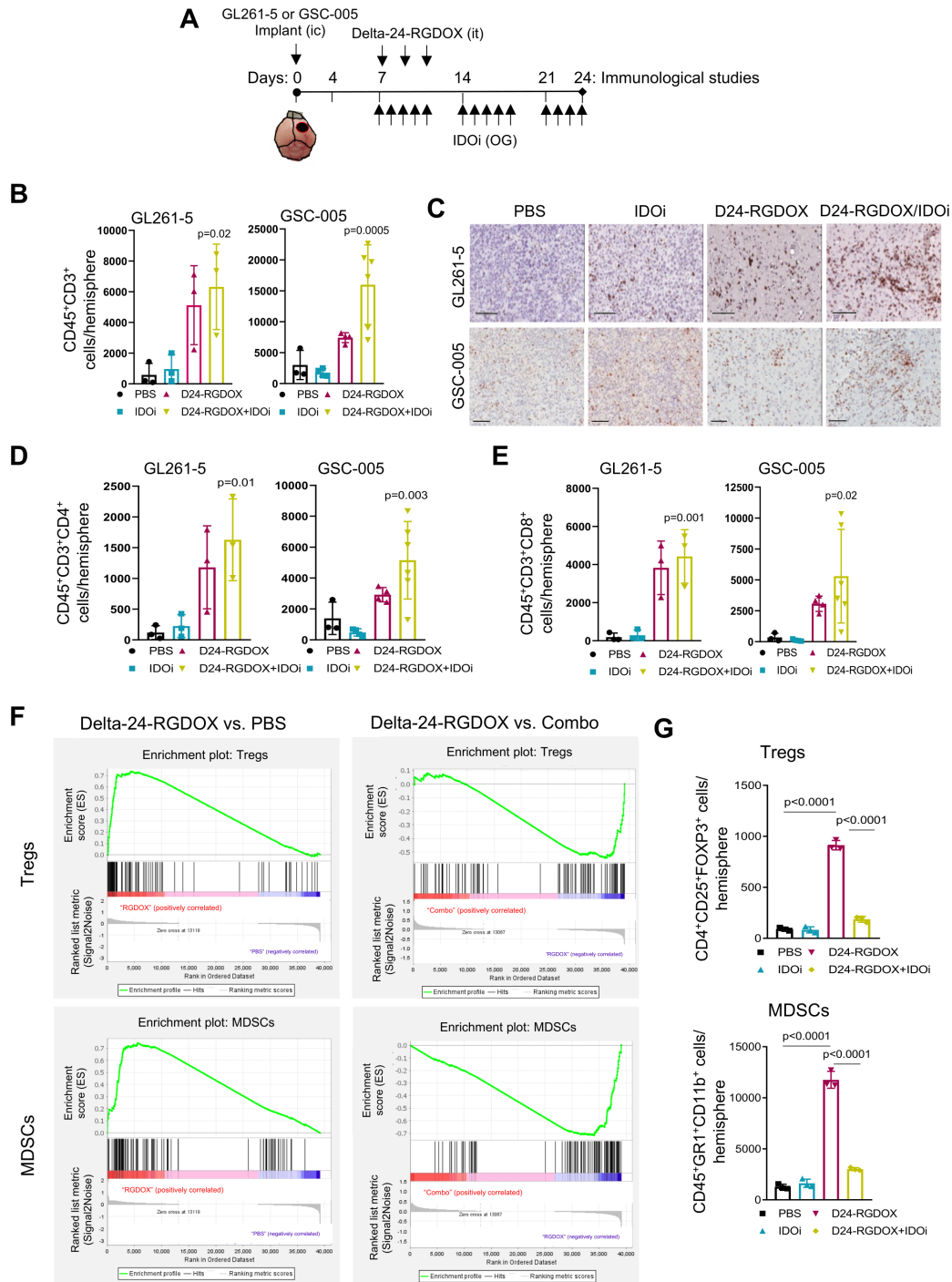


Figure 5 Combined Delta-24-RGDOX and IDO inhibitor treatment increases intratumoral T cells and decreases immunosuppressive cell populations. (A) Treatment timeline for the analysis of immune cell populations. C57BL/6 mice were intracranially (IC) implanted with GL261-5 or GSC-005 cells and randomly assigned to receive PBS (control), an IDO inhibitor (IDOi); GL261-5: indoximod. GSC-005: BGB-7204), Delta-24-RGDOX, or Delta-24-RGDOX plus IDOi. On day 24, brains were collected, stained as indicated, and analyzed using flow cytometry. Parallel experiments were performed for immunohistochemical analyses of the brains, *it*, intratumorally; *OG*, oral gavage. (B) Column graphs show the absolute numbers of CD45⁺CD3⁺ cells per tumor-containing brain hemisphere in the indicated murine glioma model. (C) Representative CD3 immunohistochemistry images for the indicated treatment groups. Images were acquired using Aperio ImageScope pathology slide viewing software. Scale bar, 100 μ m. (D, E) Column graphs show the absolute numbers of CD4⁺ (D) and CD8⁺ (E) T cells per hemisphere in the indicated murine glioma models. (F) Enrichment plots for the Treg (top) and MDSC (bottom) gene sets in PBS-treated versus Delta-24-RGDOX-treated or Delta-24-RGDOX-treated versus Combo-treated GL261-5 brain tumor RNA. (G) Column graphs show the absolute numbers of CD4⁺CD25⁺FoxP3⁺ Tregs per hemisphere (top) and CD45⁺GR1⁺CD11b⁺ MDSCs per hemisphere (bottom). Data are shown as the means \pm SDs ($n=3$). P values were derived with an ordinary one-way ANOVA (B, D–E) or a two-tailed Student's *t*-test (G). ANOVA, analysis of variance; IDO, indoleamine 2,3-dioxygenase; MDSC, myeloid-derived suppressor cell.

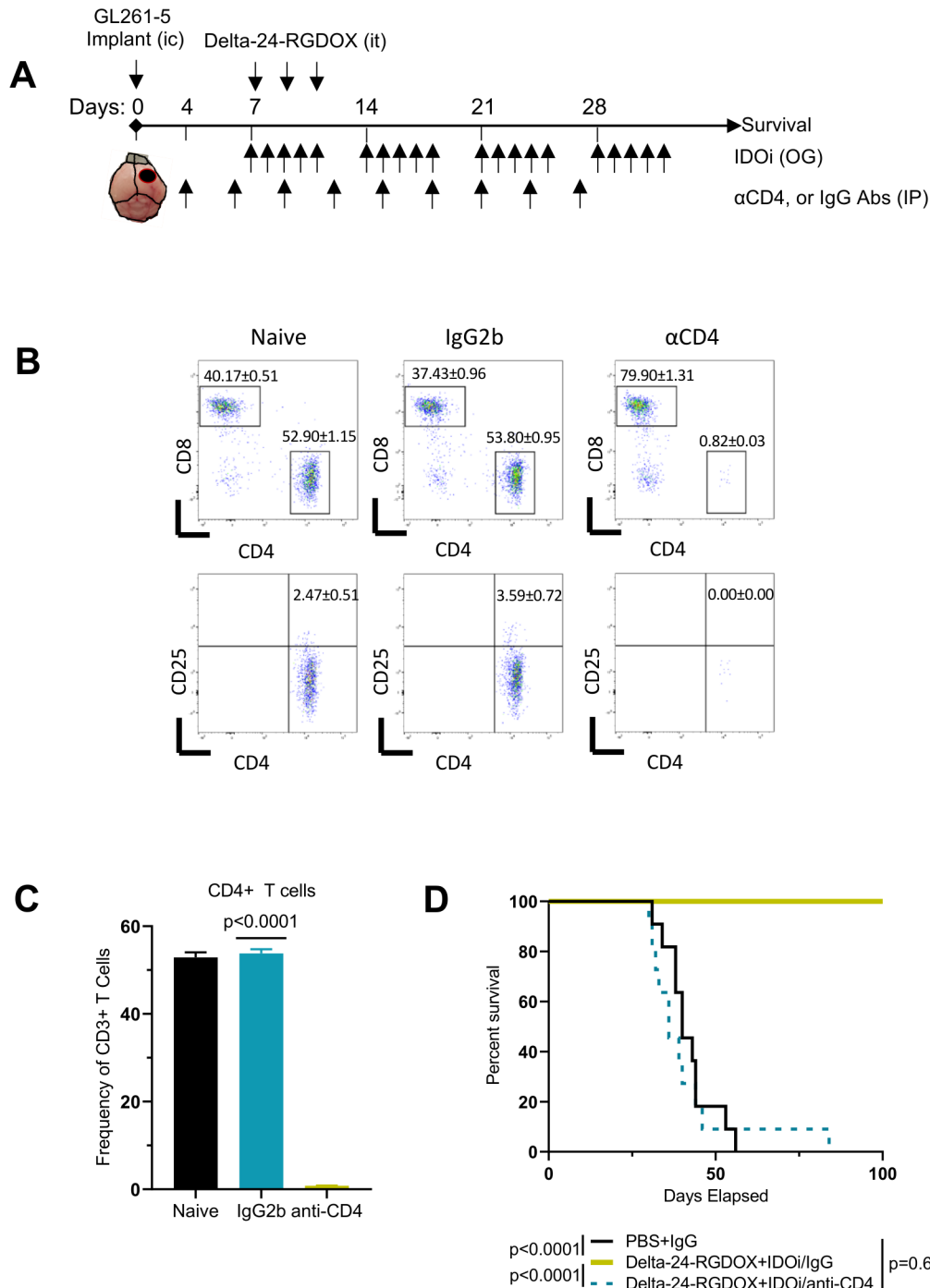


Figure 6 The therapeutic efficacy of combined Delta-24-RGDOX infection and IDO inhibition requires CD4⁺ T cell activity. (A) Treatment schedule for Delta-24-RGDOX given alone or in combination with an IDO inhibitor (IDOi) in the presence of anti-CD4 depleting antibodies. Mice were intracranially (IC) implanted with GL261-5 cells and randomly assigned to receive intratumoral (IT) injections of PBS or the combination of Delta-24-RGDOX and the IDOi indoximod ($n=10$ or 11 per group, respectively). An IgG control antibody and the anti-CD4 depleting antibodies were administered intraperitoneally. OG, oral gavage. (B) Flow cytometry plots showing CD4⁺ and CD8⁺ T cell populations in the spleen of treatment-naïve mice and mice treated with IgG2b or anti-CD4 at 38 days after tumor implantation. (C) Column graph shows the frequencies of CD4⁺ T cells in the indicated treatment groups. (D) Kaplan-Meier survival curves of GL261-5 tumor-bearing C57BL/6 mice in the different treatment groups. Data are shown as the means \pm SDs. P values were derived with a two-tailed Student's t-test (C) or the log-rank test (D). IDO, indoleamine 2,3-dioxygenase.

IFN γ and IL-2 (figure 7C). Importantly, we detected the same trend of immune activation against uninfected glioma cells (figure 7B), suggesting that tumor infection resulted in antigen spreading that led to recognition of

tumor antigens. We also evaluated immune activation at an earlier timepoint, which further confirmed the anti-tumor activation of splenocytes against uninfected cells (online supplemental figure S9).

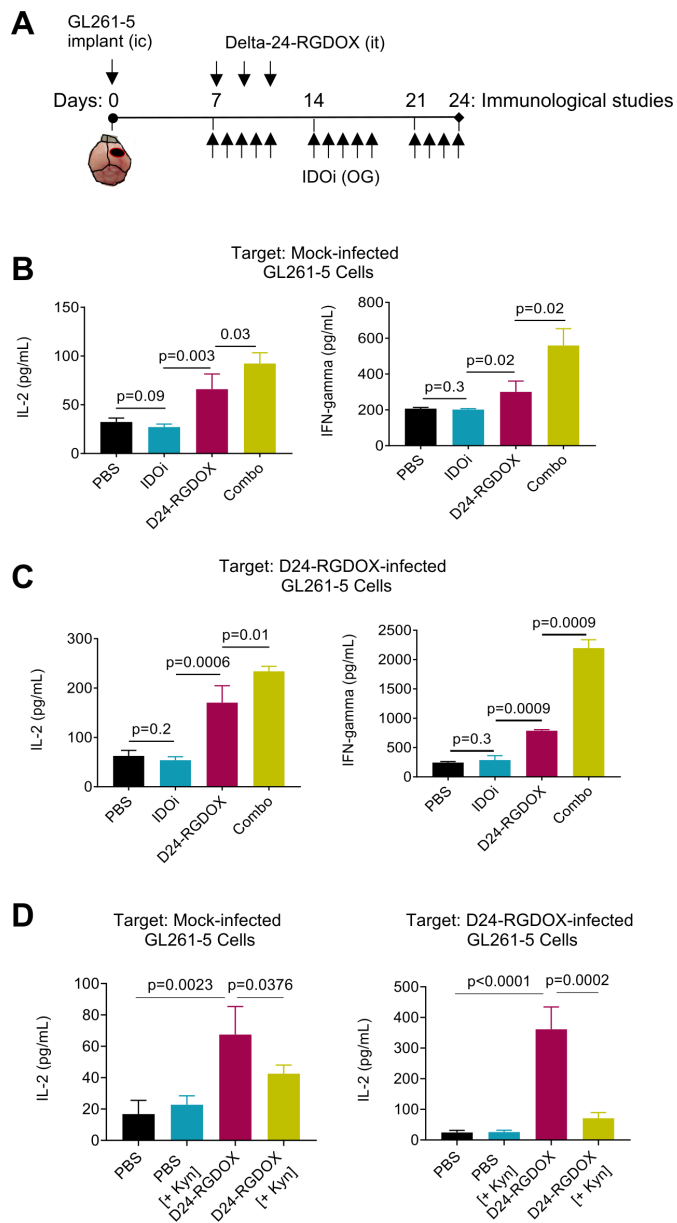


Figure 7 Combined oncolytic virus and IDO inhibitor treatment enhances antitumor immune activation. (A) Treatment timeline for the functional splenocyte assays. C57BL/6 mice were intracranially (IC) implanted with GL261-5 cells and randomly assigned to receive PBS, the IDO inhibitor (IDOi) indoximod, Delta-24-RGDOX, or Delta-24-RGDOX plus indoximod. On day 24, splenocytes from the tumor-bearing mice were cocultured with the indicated prefixed target cells for 48 hours, and the concentrations of secreted IFN γ or IL-2 were assessed by ELISA. it, intratumoral; OG, oral gavage. (B, C) Column graphs show the levels of secreted IL-2 (top) or IFN γ (bottom) in cocultures containing splenocytes from mice in the indicated treatment groups and mock-infected GL261-5 cells (B), GL261-5 cells infected with Delta-24-RGDOX (C). (D) Levels of IL-2 in co-cultures containing splenocytes from mice in the indicated groups and t mock or Delta-24-RGDOX-infected GL261-5, and the media was supplemented with kynurenine (Kyn, 25 μ M). Data are shown as the means \pm SDs (n=3). Indicated p values were evaluated using a two-tailed Student's t-test. IDO, indoleamine 2,3-dioxygenase.

We then sought to dissect the negative role of Kyn in immune activation using similar functional assays (figure 7D). To this end, we challenged the effect of IDO inhibition by enriching the culture medium with Kyn and then examined the activity of splenocytes cocultured with glioma cells.⁵¹ As expected, the secretion of IL-2 was increased in cocultures of splenocytes isolated from virus-treated mice compared with control-treated mice when either uninfected cells or virus-infected cells were included, validating the virus-induced immune activation against tumor antigens (figure 7D). Interestingly, the addition of Kyn partially decreased immune cell activation by reducing IL-2 secretion, providing evidence that Kyn had a negative effect on virus-activated splenocytes (figure 7D).⁵¹

These functional assays showed the robust effect of IDO inhibition on the activation of immune cells against cancer cells and the significant reversion of this immune activation by downstream activators of the IDO signaling circuitry. In addition, these data indirectly suggested that the IDO-Kyn circuitry has a role in counteracting the antitumoral virus-mediated immune activation.

DISCUSSION

A recent plethora of clinical trials in adults and children with brain tumors have shown that oncolytic viruses prolong the survival of a small percentage of patients (<20%).^{3 38-41} Importantly, these studies have also shown that viroimmunotherapy induces T cell infiltration into brain tumors.^{3 38-41} Such findings support the paradigm-shifting concept that complete tumor debulking by virotherapy requires the elicitation of antitumor immune responses following the initial oncolytic effect. Therefore, further enhancement of the immune arm of this treatment approach may be required to increase the percentage of positive responders,⁵² and we previously reported that the infection of a tumor with the armed oncolytic adenovirus Delta-24-RGDOX was followed by a striking activation, and significantly more robust than that triggered by the previous generation Delta-24-RGD, of the immune response in murine syngeneic models of both glioma and melanoma.^{6 7} Here, we show that RNA-seq analyses revealed that Delta-24-RGDOX infection also promoted the paradoxical activation of immunosuppressive pathways, including the IDO cascade, and immunosuppressive populations, such as Tregs and MDSCs. This double-edged activation of positive and negative immune regulators is occasionally observed during viral infections.⁵³⁻⁵⁵ As exemplified by the transcriptional signature of the treated gliomas in this study, viral infection activates immune checkpoint regulators, including CTLA-4, PD-1, and IDO.⁵⁶ This counterintuitive effect of tumor infection was confirmed by *in vitro* and *in vivo* studies showing that Delta-24-RGDOX infection is followed by the upregulation and activation of the IDO cascade, a notable finding that is in agreement with previous reports showing that IDO is upregulated in human glioma cells upon exposure

to the major antiviral cytokine IFN γ , which is also a transcriptional regulator of IDO.^{25 57} Thus, our results are consistent with the cell and tissue upregulation of IDO following cytokine stimulation in the context of infection, autoimmunity, and cancer.¹⁹

Downstream of IDO, AhR is activated by viral infection⁵⁸ and induces immunosuppression,^{11 12 59–61} which in turn can favor cancer progression. In human patients with glioblastoma, the expression of AhR is associated with a poor prognosis.⁶² Thus, the initial effect of Delta-24-RGDOX may be counteracted by the expression of the IDO-AhR cascade and the subsequent prevention of an antitumor immune response. Therefore, we hypothesized that targeting the IDO pathway should have a double-positive effect: on the one hand, improving virotherapy and, on the other hand, decreasing intrinsic tumor immunosuppression.

Of further clinical relevance, IDO and AhR are potential druggable targets in malignant gliomas.^{17 62–64} In this work, we demonstrated that Delta-24-RGDOX combined with IDO inhibitors induced prolonged survival and generated a higher rate of long-term survival than control treatments in murine models of gliomas. The addition of IDO inhibitors is required to induce anticancer effects in several models of cancer. For example, HPV16-E6-E7/HRAS-driven lung epithelial cancer was suppressed by only the combination of HPV16 E7 vaccines, OX40 agonists, and IDO inhibitors.⁶⁵ Furthermore, Berrong *et al.*⁶⁵ showed that while the addition of anti-OX40 to an antigen-specific cancer vaccine moderately enhanced therapeutic efficacy, it was the addition of an IDO inhibitor to this treatment that eventually led to complete regression of established tumors in 60% of treated mice. Additionally, in agreement with our data, Sagiv-Barfi *et al.* combined intratumoral delivery of an adenovirus-related TLR9 ligand with OX40 activation to increase anticancer T cell responses.⁶⁶

The IDO-Kyn-AhR pathway potentiates systemic toxicity during viral infection.^{32 33} Moreover, activation of the IDO-Kyn-AhR cascade worsens influenza virus infection.^{67–70} In addition, constitutive AhR activation reduces the type I IFN antiviral response.²⁴ Based on these data, although in this study we did not observe any sign of toxicity, the inhibition of the IDO circuitry should likely limit the potential systemic toxicity of Delta-24-RGDOX in clinical trials.

The OX40 pathway is predominantly active in CD4⁺ T cells.⁷¹ In our models, the anticancer effect of Delta-24-RGDOX infection combined with IDO inhibition was due to the elicitation of a robust antitumor immune response. Thus, we observed increased absolute counts of tumor infiltrating CD4⁺ and CD8⁺ T lymphocytes in combination treated tumors. These observations aligned with our functional studies showing that Kyn negatively regulated T cell responses to viral or tumor antigens. Furthermore, antibody depletion of CD4⁺ T cells abolished the antitumor effect of the combination therapy, indicating that

the T helper cell response is required to elicit antitumor immune responses.

Our data also indicated that the virus-mediated upregulation of the IDO cascade was associated with intriguing increases in the MDSC and Treg populations, which were partially counteracted by IDO inhibition. In this regard, IDO orchestrates in solid tumors immunosuppressive effects through Treg-dependent recruitment and activation of MDSCs,⁴⁷ which can be reversed by IDO inhibition.⁴⁷ Moreover, IDO activity inhibits the proliferation of antigen-specific T lymphocytes, inducing tumor tolerance,^{61 72–75} and further inhibits T cell-based adaptive immunity by promoting the differentiation of Tregs in tumors,^{15 76–78} which can be induced by Kyn¹¹ and result in the suppression of antigen-specific T cell responses.^{51 79} It is important to note that in our cell system, the addition of Kyn to cocultures of splenocytes from treated mice and cancer cells efficiently suppressed the activation of the immune cells elicited by Delta-24-RGDOX.

In conclusion, our findings reveal that immunosuppressive pathways play a prominent role in the resistance of solid tumors to oncolytic virotherapy. Furthermore, the activity of the tumor microenvironment IDO circuitry is responsible, at least partially, for the remodeling of local immunosuppression after tumor infection. Combining molecular and immune-related therapies may improve outcomes in human gliomas and other cancers treated with virotherapy. These highly translatable studies should propel the development of a clinical trial to test the safety and efficacy of the combination of oncolytic adenoviruses armed with T cell activators and IDO inhibitors in patients with glioblastoma and other solid tumors.

Author affiliations

¹Department of Neuro-Oncology, The University of Texas MD Anderson Cancer Center, Houston, Texas, USA

²The University of Texas MD Anderson Cancer Center UTHealth Graduate School of Biomedical Sciences, Houston, Texas, USA

³Department of Neurosurgery, The University of Texas MD Anderson Cancer Center, Houston, Texas, USA

⁴Department of Microbiology and Medical Zoology, University of Puerto Rico School of Medicine, San Juan, Puerto Rico

⁵The University of Texas Health Science Center at Houston School of Biomedical Informatics, Houston, Texas, USA

⁶Department of Neurological Surgery, Northwestern University Feinberg School of Medicine, Chicago, Illinois, USA

⁷Pediatrics, Clínica Universidad de Navarra, Pamplona, Spain

⁸Program of Solid Tumors, CIMBA, Pamplona, Spain

⁹Department of Medicine-Hematology/Oncology, Northwestern University Feinberg School of Medicine, Chicago, Illinois, USA

Twitter Hong Jiang @HongJia15477637, Marta M Alonso @pumorister and Derek A Wainwright @dwainwright_PhD

Acknowledgements The authors thank Dr. Inder M. Verma (The Salk Institute for Biological Studies, La Jolla, CA, USA) for generously providing the GSC-005 glioma culture; Verlene Henry for providing technical assistance with animal experiments; Drs. William K. Russel and Rahul Deshpande (Mass Spectrometry Facility, University of Texas Medical Branch at Galveston, TX, USA) for performing the liquid chromatography–mass spectrometry analysis; and Joseph Munch, Mark Picus, and Stephanie Deming (Editing Services in MD Anderson Cancer Center Research Medical Library) for their assistance in language editing of this manuscript.

Contributors Conceptualization and design: TN, HJ, FL, MA, DW, CG-M, and JF. Development of methodology and acquisition of data: TN, DHS, SS, YR-M, XF, JG, LZ, EL, and KLL. Data analysis: TN, SKS, HJ, SS, CA-B, FG-V, LZ, and WJZ. Supervision: CG-M, JF. Writing, review, revision, and guarantors of the manuscript: TN, CG-M, and JF.

Funding This work was supported by the National Institutes of Health (NIH) F31CA228207 (TN), R01CA256006 (JF, CG-M), P50CA127001 (JF, FL), 1UL1TR003167 (WJZ), R01AG066749 (WJZ) and U54CA096297 (CG-M, FG-V); The University of Texas MD Anderson Cancer Center Glioblastoma Moon Shots Program (FL, CG-M, JF); James P. Harris Brain Tumor Research Fund; Bradley Zankel Foundation (JF); and John and Rebekah Harper Fellowship (DHS). This study also used MD Anderson's Research Animal Support Facility and Advanced Technology Genomics Core, which are supported in part by the NIH/NCI through MD Anderson's Cancer Center Support Grant P30CA01667, and the Cancer Prevention and Research Institute of Texas (CPRIT) RP170668 (WJZ) and RP190682 (supporting the Mass Spectrometry Facility at the University of Texas Medical Branch, Galveston, TX).

Disclaimer The funding bodies were not involved in the study design, the data collection and analysis, the decision to publish, or the preparation of the manuscript.

Competing interests MA, HJ, FL, CG-M, and JF report license agreements with DNAtrix. CG-M and JF are shareholders of DNAtrix. MA reports DNAtrix-sponsored research not related to this work.

Patient consent for publication Not applicable.

Ethics approval Not applicable.

Provenance and peer review Not commissioned; externally peer reviewed.

Data availability statement All data relevant to the study are included in the article or uploaded as online supplemental information.

Supplemental material This content has been supplied by the author(s). It has not been vetted by BMJ Publishing Group Limited (BMJ) and may not have been peer-reviewed. Any opinions or recommendations discussed are solely those of the author(s) and are not endorsed by BMJ. BMJ disclaims all liability and responsibility arising from any reliance placed on the content. Where the content includes any translated material, BMJ does not warrant the accuracy and reliability of the translations (including but not limited to local regulations, clinical guidelines, terminology, drug names and drug dosages), and is not responsible for any error and/or omissions arising from translation and adaptation or otherwise.

Open access This is an open access article distributed in accordance with the Creative Commons Attribution Non Commercial (CC BY-NC 4.0) license, which permits others to distribute, remix, adapt, build upon this work non-commercially, and license their derivative works on different terms, provided the original work is properly cited, appropriate credit is given, any changes made indicated, and the use is non-commercial. See <http://creativecommons.org/licenses/by-nc/4.0/>.

ORCID iDs

Sagar Sohoni <http://orcid.org/0000-0002-4041-2937>

Hong Jiang <http://orcid.org/0000-0003-4668-5319>

Marta M Alonso <http://orcid.org/0000-0002-7520-7351>

Derek A Wainwright <http://orcid.org/0000-0001-7232-4264>

Juan Fueyo <http://orcid.org/0000-0001-6941-2335>

REFERENCES

- Challenor S, Tucker D. SARS-CoV-2-induced remission of Hodgkin lymphoma. *Br J Haematol* 2021;192:415.
- Sollini M, Gelardi F, Carlo-Stella C. Complete remission of follicular lymphoma after SARS-CoV-2 infection: from the "flare phenomenon" to the "abscopal effect. *Eur J Nucl Med Mol Imaging* 2021.
- Lang FF, Conrad C, Gomez-Manzano C, et al. Phase I study of DNx-2401 (Delta-24-RGD) oncolytic adenovirus: replication and immunotherapeutic effects in recurrent malignant glioma. *J Clin Oncol* 2018;36:JCO2017758219.
- Jiang H, Fueyo J. Healing after death: antitumor immunity induced by oncolytic adenoviral therapy. *Oncoimmunology* 2014;3:e947872.
- Jiang H, Gomez-Manzano C, Rivera-Molina Y, et al. Oncolytic adenovirus research evolution: from cell-cycle checkpoints to immune checkpoints. *Curr Opin Virol* 2015;13:33–9.
- Jiang H, Rivera-Molina Y, Gomez-Manzano C, et al. Oncolytic adenovirus and tumor-targeting immune modulatory therapy improve autologous cancer vaccination. *Cancer Res* 2017;77:3894–907.
- Jiang H, Shin DH, Nguyen TT, et al. Localized treatment with oncolytic adenovirus Delta-24-RGDOX induces systemic immunity against disseminated subcutaneous and intracranial melanomas. *Clin Cancer Res* 2019;25:6801–14.
- Saleh R, Elkord E. Acquired resistance to cancer immunotherapy: role of tumor-mediated immunosuppression. *Semin Cancer Biol* 2020;65:13–27.
- Schmidt SV, Schultze JL. New insights into IDO biology in bacterial and viral infections. *Front Immunol* 2014;5:384.
- Uyttenhove C, Pilotte L, Théate I, et al. Evidence for a tumoral immune resistance mechanism based on tryptophan degradation by indoleamine 2,3-dioxygenase. *Nat Med* 2003;9:1269–74.
- Mezrich JD, Fechner JH, Zhang X, et al. An interaction between kynurenine and the aryl hydrocarbon receptor can generate regulatory T cells. *J Immunol* 2010;185:3190–8.
- Quintana FJ, Basso AS, Iglesias AH, et al. Control of T(reg) and T(H)17 cell differentiation by the aryl hydrocarbon receptor. *Nature* 2008;453:65–71.
- Routy J-P, Routy B, Graziani GM, et al. The kynurenine pathway is a double-edged sword in Immune-Privileged sites and in cancer: implications for immunotherapy. *Int J Tryptophan Res* 2016;9:67–77.
- Munn DH, Sharma MD, Hou D, et al. Expression of indoleamine 2,3-dioxygenase by plasmacytoid dendritic cells in tumor-draining lymph nodes. *J Clin Invest* 2004;114:280–90.
- Curti A, Pandolfi S, Valzasina B, et al. Modulation of tryptophan catabolism by human leukemic cells results in the conversion of CD25⁺ into CD25⁺ T regulatory cells. *Blood* 2007;109:2871–7.
- Mansfield AS, Heikkilä PS, Vaara AT, et al. Simultaneous FOXP3 and IDO expression is associated with sentinel lymph node metastases in breast cancer. *BMC Cancer* 2009;9:231.
- Wainwright DA, Balyasnikova IV, Chang AL, et al. IDO expression in brain tumors increases the recruitment of regulatory T cells and negatively impacts survival. *Clin Cancer Res* 2012;18:6110–21.
- Du L, Xing Z, Tao B, et al. Both IDO1 and TDO contribute to the malignancy of gliomas via the Kyn-AhR-AQP4 signaling pathway. *Signal Transduct Target Ther* 2020;5:10.
- Jaronen M, Quintana FJ. Immunological relevance of the coevolution of IDO1 and AHR. *Front Immunol* 2014;5:521.
- Ladomersky E, Zhai L, Lenzen A, et al. IdO1 inhibition synergizes with radiation and PD-1 blockade to durably increase survival against advanced glioblastoma. *Clin Cancer Res* 2018;24:2559–73.
- Labadie BW, Bao R, Luke JJ. Reimagining IDO pathway inhibition in cancer immunotherapy via downstream focus on the Tryptophan-Kynurenine-Aryl hydrocarbon axis. *Clin Cancer Res* 2019;25:1462–71.
- Platten M, von Knebel Doeberitz N, Oezen I, et al. Cancer immunotherapy by targeting IDO1/TDO and their downstream effectors. *Front Immunol* 2015;5:673.
- Litzenburger UM, Opitz CA, Sahm F, et al. Constitutive IDO expression in human cancer is sustained by an autocrine signaling loop involving IL-6, STAT3 and the AhR. *Oncotarget* 2014;5:1038–51.
- Yamada T, Horimoto H, Kameyama T, et al. Constitutive aryl hydrocarbon receptor signaling constrains type I interferon-mediated antiviral innate defense. *Nat Immunol* 2016;17:687–94.
- Yoshida R, Imanishi J, Oku T, et al. Induction of pulmonary indoleamine 2,3-dioxygenase by interferon. *Proc Natl Acad Sci U S A* 1981;78:129–32.
- Arumuggam N, Bhowmick NA, Rupasinghe HPV. A review: phytochemicals targeting JAK/STAT signaling and IDO expression in cancer. *Phytother Res* 2015;29:805–17.
- Boasso A, Hardy AW, Anderson SA, et al. HIV-induced type I interferon and tryptophan catabolism drive T cell dysfunction despite phenotypic activation. *PLoS One* 2008;3:e2961.
- Schroeksnadel K, Zangerle R, Bellmann-Weiler R, et al. Indoleamine-2, 3-dioxygenase and other interferon-gamma-mediated pathways in patients with human immunodeficiency virus infection. *Curr Drug Metab* 2007;8:225–36.
- Sage LK, Fox JM, Mellor AL, et al. Indoleamine 2,3-dioxygenase (IDO) activity during the primary immune response to influenza infection modifies the memory T cell response to influenza challenge. *Viral Immunol* 2014;27:112–23.
- Zhai L, Spranger S, Binder DC, et al. Molecular pathways: targeting IDO1 and other tryptophan dioxygenases for cancer immunotherapy. *Clin Cancer Res* 2015;21:5427–33.
- Murray IA, Patterson AD, Perdew GH. Aryl hydrocarbon receptor ligands in cancer: friend and foe. *Nat Rev Cancer* 2014;14:801–14.
- Barroso A, Gualdrón-López M, Esper L, et al. The aryl hydrocarbon receptor modulates production of cytokines and reactive oxygen species and development of myocarditis during *Trypanosoma cruzi* infection. *Infect Immun* 2016;84:3071–82.

- 33 Sanchez Y, Rosado JdeD, Vega L, *et al.* The unexpected role for the aryl hydrocarbon receptor on susceptibility to experimental toxoplasmosis. *J Biomed Biotechnol* 2010;2010:1–15.
- 34 Gutiérrez-Vázquez C, Quintana FJ. Regulation of the immune response by the aryl hydrocarbon receptor. *Immunity* 2018;48:19–33.
- 35 Rothhammer V, Quintana FJ. The aryl hydrocarbon receptor: an environmental sensor integrating immune responses in health and disease. *Nat Rev Immunol* 2019;19:184–97.
- 36 Munn DH, Mellor AL. Indoleamine 2,3 dioxygenase and metabolic control of immune responses. *Trends Immunol* 2013;34:137–43.
- 37 Prendergast GC, Mondal A, Dey S, *et al.* Inflammatory Reprogramming with IDO1 Inhibitors: Turning Immunologically Unresponsive 'Cold' Tumors 'Hot'. *Trends Cancer* 2018;4:38–58.
- 38 Friedman GK, Johnston JM, Bag AK, *et al.* Oncolytic HSV-1 G207 Immunovirotherapy for pediatric high-grade gliomas. *N Engl J Med* 2021;384:1613–22.
- 39 Cloughesy TF, Landolfi J, Hogan DJ, *et al.* Phase 1 trial of vocimagene amiretrorepvec and 5-fluorocytosine for recurrent high-grade glioma. *Sci Transl Med* 2016;8:ra375.
- 40 Desjardins A, Gromeier M, Herndon JE, *et al.* Recurrent glioblastoma treated with recombinant poliovirus. *N Engl J Med* 2018;379:150–61.
- 41 Markert JM, Razdan SN, Kuo H-C, *et al.* A phase 1 trial of oncolytic HSV-1, G207, given in combination with radiation for recurrent GBM demonstrates safety and radiographic responses. *Mol Ther* 2014;22:1048–55.
- 42 Brown CE, Badie B, Barish ME, *et al.* Bioactivity and safety of IL13R α 2-Redirected chimeric antigen receptor CD8+ T cells in patients with recurrent glioblastoma. *Clin Cancer Res* 2015;21:4062–72.
- 43 Ahmed N, Brawley V, Hegde M, *et al.* HER2-Specific chimeric antigen receptor-modified virus-specific T cells for progressive glioblastoma: a phase 1 dose-escalation trial. *JAMA Oncol* 2017;3:1094–101.
- 44 O'Rourke DM, Nasrallah MP, Desai A, *et al.* A single dose of peripherally infused EGFRvIII-directed CAR T cells mediates antigen loss and induces adaptive resistance in patients with recurrent glioblastoma. *Sci Transl Med* 2017;9. doi:10.1126/scitranslmed.aaa0984. [Epub ahead of print: 19 07 2017].
- 45 Ott PA, Bang Y-J, Piha-Paul SA, *et al.* T-Cell-Inflamed gene-expression profile, programmed death ligand 1 expression, and tumor mutational burden predict efficacy in patients treated with pembrolizumab across 20 cancers: KEYNOTE-028. *J Clin Oncol* 2019;37:318–27.
- 46 Kurz SC, Cabrera LP, Hastie D, *et al.* PD-1 inhibition has only limited clinical benefit in patients with recurrent high-grade glioma. *Neurology* 2018;91:e1355–9.
- 47 Holmgaard RB, Zamarin D, Li Y, *et al.* Tumor-Expressed IDO recruits and activates MDSCs in a Treg-Dependent manner. *Cell Rep* 2015;13:412–24.
- 48 Burchill MA, Yang J, Vogtenhuber C, *et al.* IL-2 receptor beta-dependent STAT5 activation is required for the development of Foxp3+ regulatory T cells. *J Immunol* 2007;178:280–90.
- 49 Owen DL, Mahmud SA, Sjaastad LE, *et al.* Thymic regulatory T cells arise via two distinct developmental programs. *Nat Immunol* 2019;20:195–205.
- 50 Croft M, So T, Duan W, *et al.* The significance of OX40 and OX40L to T-cell biology and immune disease. *Immunol Rev* 2009;229:173–91.
- 51 Dagenais-Lussier X, Aounallah M, Mehraj V, *et al.* Kynurenine reduces memory CD4 T-cell survival by interfering with interleukin-2 signaling early during HIV-1 infection. *J Virol* 2016;90:7967–79.
- 52 Sharma P, Allison JP. The future of immune checkpoint therapy. *Science* 2015;348:56–61.
- 53 Cao S, Wylie KM, Wyczalkowski MA, *et al.* Dynamic host immune response in virus-associated cancers. *Commun Biol* 2019;2:109.
- 54 Viganò S, Perreau M, Pantaleo G, *et al.* Positive and negative regulation of cellular immune responses in physiologic conditions and diseases. *Clin Dev Immunol* 2012;2012:1–11.
- 55 Goldszmid RS, Dzutsev A, Trinchieri G. Host immune response to infection and cancer: unexpected commonalities. *Cell Host Microbe* 2014;15:295–305.
- 56 Wykes MN, Lewin SR. Immune checkpoint blockade in infectious diseases. *Nat Rev Immunol* 2018;18:91–104.
- 57 Yoshida R, Urade Y, Tokuda M, *et al.* Induction of indoleamine 2,3-dioxygenase in mouse lung during virus infection. *Proc Natl Acad Sci U S A* 1979;76:4084–6.
- 58 Giovannoni F, Li Z, Garcia CC, *et al.* A potential role for AHR in SARS-CoV-2 pathology. *Res Sq* 2020. doi:10.21203/rs.3.rs-25639/v1. [Epub ahead of print: 27 Apr 2020].
- 59 Terness P, Bauer TM, Röse L, *et al.* Inhibition of allogeneic T cell proliferation by indoleamine 2,3-dioxygenase-expressing dendritic cells: mediation of suppression by tryptophan metabolites. *J Exp Med* 2002;196:447–57.
- 60 Fallarino F, Grohmann U, Vacca C, *et al.* T cell apoptosis by tryptophan catabolism. *Cell Death Differ* 2002;9:1069–77.
- 61 Frumento G, Rotondo R, Tonetti M, *et al.* Tryptophan-derived catabolites are responsible for inhibition of T and natural killer cell proliferation induced by indoleamine 2,3-dioxygenase. *J Exp Med* 2002;196:459–68.
- 62 Takenaka MC, Gabriely G, Rothhammer V, *et al.* Control of tumor-associated macrophages and T cells in glioblastoma via AHR and CD39. *Nat Neurosci* 2019;22:729–40.
- 63 Perepechaeva ML, Grishanova AY. The role of aryl hydrocarbon receptor (Ahr) in brain tumors. *Int J Mol Sci* 2020;21. doi:10.3390/ijms21082863. [Epub ahead of print: 20 Apr 2020].
- 64 Zhai L, Lauing KL, Chang AL, *et al.* The role of IDO in brain tumor immunotherapy. *J Neurooncol* 2015;123:395–403.
- 65 Berrong Z, Mkrtchyan M, Ahmad S, *et al.* Antigen-specific antitumor responses induced by OX40 agonist are enhanced by the IDO inhibitor Indoximod. *Cancer Immunol Res* 2018;6:201–8.
- 66 Sagiv-Barfi I, Czerwinski DK, Levy S, *et al.* Eradication of spontaneous malignancy by local immunotherapy. *Sci Transl Med* 2018;10. doi:10.1126/scitranslmed.aan4488. [Epub ahead of print: 31 01 2018].
- 67 Jin G-B, Moore AJ, Head JL, *et al.* Aryl hydrocarbon receptor activation reduces dendritic cell function during influenza virus infection. *Toxicol Sci* 2010;116:514–22.
- 68 Jin G-B, Winans B, Martin KC, *et al.* New insights into the role of the aryl hydrocarbon receptor in the function of CD11c⁺ cells during respiratory viral infection. *Eur J Immunol* 2014;44:1685–98.
- 69 Lawrence BP, Roberts AD, Neumiller JJ, *et al.* Aryl hydrocarbon receptor activation impairs the priming but not the recall of influenza virus-specific CD8+ T cells in the lung. *J Immunol* 2006;177:5819–28.
- 70 Warren TK, Mitchell KA, Lawrence BP. Exposure to 2,3,7,8-tetrachlorodibenzo-p-dioxin (TCDD) suppresses the humoral and cell-mediated immune responses to influenza A virus without affecting cytolytic activity in the lung. *Toxicol Sci* 2000;56:114–23.
- 71 Croft M. Control of immunity by the TNFR-related molecule OX40 (CD134). *Annu Rev Immunol* 2010;28:57–78.
- 72 Grohmann U, Fallarino F, Puccetti P. Tolerance, DCs and tryptophan: much ado about IDO. *Trends Immunol* 2003;24:242–8.
- 73 Mellor AL, Keskin DB, Johnson T, *et al.* Cells expressing indoleamine 2,3-dioxygenase inhibit T cell responses. *J Immunol* 2002;168:3771–6.
- 74 Sznurkowski JJ, Zawrocki A, Emerich J, *et al.* Expression of indoleamine 2,3-dioxygenase predicts shorter survival in patients with vulvar squamous cell carcinoma (vSCC) not influencing on the recruitment of FOXP3-expressing regulatory T cells in cancer nests. *Gynecol Oncol* 2011;122:307–12.
- 75 Munn DH, Shafiqzadeh E, Attwood JT, *et al.* Inhibition of T cell proliferation by macrophage tryptophan catabolism. *J Exp Med* 1999;189:1363–72.
- 76 Curti A, Trabanelli S, Salvestrini V, *et al.* The role of indoleamine 2,3-dioxygenase in the induction of immune tolerance: focus on hematology. *Blood* 2009;113:2394–401.
- 77 Curti A, Trabanelli S, Onofri C, *et al.* Indoleamine 2,3-dioxygenase-expressing leukemic dendritic cells impair a leukemia-specific immune response by inducing potent T regulatory cells. *Haematologica* 2010;95:2022–30.
- 78 Levina V, Su Y, Gorelik E. Immunological and nonimmunological effects of indoleamine 2,3-dioxygenase on breast tumor growth and spontaneous metastasis formation. *Clin Dev Immunol* 2012, 173029 2012.
- 79 Platten M, Ho PP, Youssef S, *et al.* Treatment of autoimmune neuroinflammation with a synthetic tryptophan metabolite. *Science* 2005;310:850–5.